Superconducting Bardeen-Cooper-Schrieffer versus Fulde-Ferrell-Larkin-Ovchinnikov states of heavy quasiparticles with spin-dependent masses and Kondo-type pairing

M. M. Maśka[*]

Institute of Physics, University of Silesia, Uniwersytecka 4, 40-007 Katowice, Poland

M. Mierzejewski

Institute of Physics, University of Silesia, Uniwersytecka 4, 40-007 Katowice, Poland
and J. Stefan Institute, SI-1000 Ljubljana, Slovenia

J. Kaczmarczyk

Marian Smoluchowski Institute of Physics, Jagiellonian University, Reymonta 4, 30-059 Kraków, Poland

J. Spałek[†]

Marian Smoluchowski Institute of Physics, Jagiellonian University, Reymonta 4, 30-059 Kraków, Poland
and Faculty of Physics and Applied Computer Science, AGH University of Science and Technology,
Reymonta 19, 30-059 Kraków, Poland

The observation of the Fulde-Ferrell-Larkin-Ovchinnikov (FFLO) superconducting state and detection of the spin-dependent effective masses (SDM) of quasiparticles in heavy-fermion systems are combined into a single theoretical framework within the (mean-field) Gutzwiller approximation for the correlated states of electrons on a two-dimensional square lattice. The tight-binding approximation with nonzero first two hopping integrals is assumed for the bare electrons. The appearance of the spin-split masses extends essentially the regime of temperatures and applied magnetic fields in which FFLO (of the homogeneous, Fulde-Ferrell form) is stable and thus is claimed to be very important for its detectability. The analysis is performed within the Kondo-lattice limit of the finite-U Anderson–lattice model accounting in a coherent manner for both the mass renormalization (in the Gutzwiller approximation) and real-space pairing among the correlated heavy quasiparticles, the latter driven by the Kondo-type exchange interaction. The results are compared briefly with those obtained recently for a simpler situation of interacting fermion gas treated within a similar scheme. In Appendices A and B the Kondo real-space pairing and the Bogolyubov transformation for the SDM case are detailed.

I. INTRODUCTION

Among new superconductors discovered at the beginning of this decade are those termed as *unconventional*, i.e., those which exhibit breakdown of basic symmetries such as the spatial inversion[1] or the time reversal,[2] as well as the singlet-triplet Cooper pair mixing.[3] These features have been observed in heavy-fermion compounds[4] and demonstrate a *nonstandard* behavior even when the Bogolyubov-Valatin-de Gennes quasiparticle approach can still be applied. Such an approach is based on the concept of Landau-Fermi liquid, which in the present situation is called *almost localized*.[5] By almost localized Fermi liquid we understand first of all a fermionic liquid with large and spin-dependent mass (SDM) enhancement in the magnetically polarized state. Such liquid is realized in a system with the band filling of the uppermost valence band close to that corresponding to the Mott-Hubbard insulator (i.e., close to an integer value). A separate, largely unanswered question is concerned with the pairing in the non-Fermi (non-Landau) liquids[6] and particularly, in high-temperature superconductors.[7]

Under these circumstances, it seems proper to select the cases, for which a limited number of novel factors such as the spin dependence of quasiparticle mass[8–11] and the real-space pairing induced by strong correlations[12] can be incorporated into an effective Fermi-liquid picture. In such situation the whole problem becomes tractable within modified Bardeen, Cooper, and Schrieffer (BCS) theory in the form of extended Bogolyubov-Valatin-de Gennes-Nambu approach. All these topics constitute the contents of the present paper. Explicitly, we consider a two-dimensional (square) lattice model of correlated electrons treated within the Gutzwiller approach to correlated states[13] and calculate the phase diagram encompassing both the BCS and the Fulde-Ferrell-Larkin-Ovchinnikov (FFLO) states in an applied magnetic field in the Pauli-limiting case which is appropriate for the heavy-fermion systems. This paper thus proposes a modified Fermi-liquid description of an unconventional superconductor with strongly correlated electrons which lead to SDMs and real-space pairing induced by exchange interactions. In connection with this one should note that the concept of SDM has been also used recently in the context of coexistence of ferromagnetism and superconductivity.[14]

The structure of the paper is as follows. In Sec. II we introduce briefly the narrow-band limit of the Anderson-lattice model with real-space hybrid pairing[12] among the correlated particles in the Gutzwiller-projected state. We also introduce there a basic description of the paired state within the properly modified BCS approach for the renormalized mean-field state. In Sec. III we present detailed numerical

results concerning the quasiparticle states, as well as the phase diagram including the simplest, homogeneous, type (Fulde-Ferrell, FF) of the possible FFLO states. We show there that the inclusion of the spin dependence of quasiparticle masses[8–11] stabilizes the FFLO state in much wider interval of temperature and applied field. This result is related to the discovery[10] of SDM in the CeCoIn$_5$ system, in which the FFLO phase was proposed,[15] most probably mixed with antiferromagnetism.[16] In Sec. IV we overview briefly the whole approach and compare our results with those obtained recently for a simpler situation of interacting fermion gas treated within a similar scheme. In Appendix A we provide a detailed discussion of the Kondo-type pairing and in Appendix B define the Bogolyubov quasiparticles, as well as sketch the solution for the superconducting states with SDM in the magnetically polarized state within the self-consistent BCS approach.

II. MODEL

As mentioned already, the goal of this paper is to incorporate the spin-dependent quasiparticle masses (Refs. 8–11) of heavy electrons into the description of superconductivity. The heavy electrons are treated in the tight-binding approximation for the two-dimensional square lattice. We analyze in detail a relative stability of the BCS phase against the FF type of FFLO state in an applied magnetic field **H** and at temperature $T \geq 0$. We introduce also the Kondo-type real-space pairing for the finite-U Anderson lattice, as it constitutes a coherent part of the whole problem studied.

A. Effective Anderson-lattice Hamiltonian with Kondo-type real-space pairing

We start with the effective Anderson-lattice Hamiltonian in the large, but finite-U limit, which in the Wannier representation has the form (cf. also Appendix A)

$$H = \sum_{mn\sigma} (t_{mn}^{(c)} - \mu\delta_{mn})c_{m\sigma}^\dagger c_{n\sigma} + (\epsilon_f - \mu)\sum_{i\sigma} N_{i\sigma}(1 - N_{i\bar\sigma})$$
$$+ \sum_{im\sigma} V_{im}(1 - N_{i\bar\sigma})(f_{i\sigma}^\dagger c_{m\sigma} + c_{m\sigma}^\dagger f_{i\sigma}) - 2\sum_{imn} \frac{2V_{im}V_{in}}{U + \epsilon_f} b_{im}^\dagger b_{in}.$$
$$(1)$$

In this Hamiltonian the doubly occupied f-electron atomic states have been projected out. The first term represents the conduction (c) electrons (with the chemical-potential part subtracted), the second describes the originally localized (f) electrons with the site double occupancies projected out (the corresponding number operator is $N_{i\sigma} \equiv f_{i\sigma}^\dagger f_{i\sigma}$), the third—the projected f-c hybridization, and the fourth the real-space pairing part in the leading order [cf. Figs. 1(a) and 1(b)] with the projected spin-singlet hybrid pairing operators

$$b_{im}^\dagger \equiv \frac{1}{\sqrt{2}}[f_{i\uparrow}^\dagger(1 - N_{i\downarrow})c_{m\downarrow}^\dagger - f_{i\downarrow}^\dagger(1 - N_{i\uparrow})c_{m\uparrow}^\dagger], \quad b_{im} \equiv (b_{im}^\dagger)^\dagger.$$
$$(2)$$

The above real-space operators are intrasite if $V_{im} = V\delta_{im}$, i.e., the hybridization has an intra-atomic nature. The pairing part
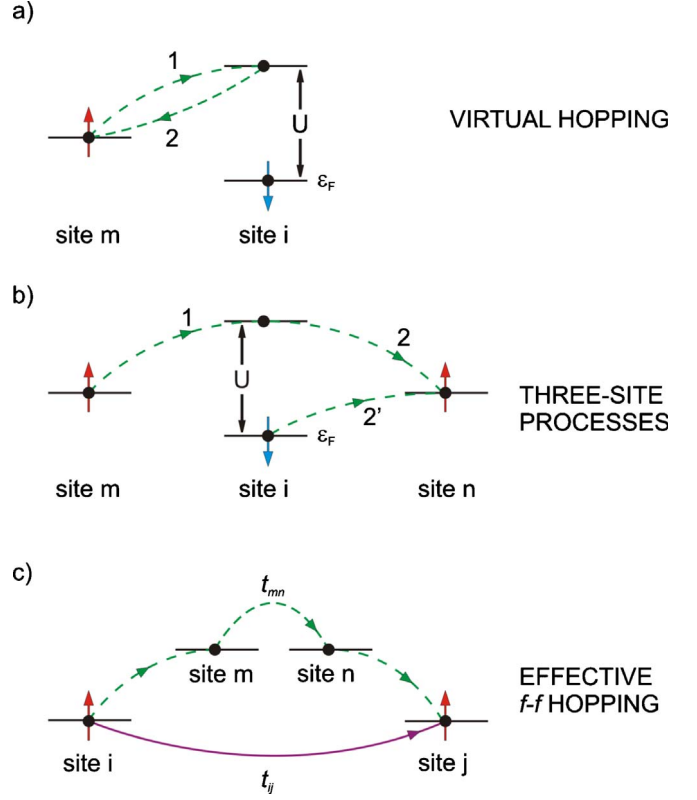
FIG. 1. (Color online) Schematic representation of the hoppings processes to second order in V_{im}. The hopping labeled as 2 and 2′ in (b) are alternative processes. The processes (a) and (b) lead to real-space pairing, whereas the three-step process (c) leads to the itineracy of the originally atomic f electrons with effective hopping t_{ij}. All three processes contribute to the dynamics of heavy quasiparticles with renormalized characteristics. The processes are discussed in analytic terms in main text and Appendix A. The virtual process (a) leads to the Kondo interaction, whereas the process (b) introduces hybrid pair hopping.

disappears if the f-f intra-atomic (Hubbard) interaction $U \to \infty$. For $U < \infty$ the hybrid pairing represents a part of Kondo-type interaction which is derived[12] in direct analogy to the pairing represented by t-J model.[7,17] Note that the Kondo part contains only the "high-energy" virtual hopping processes (with f-site double occupancies in the intermediate state), not the full Schrieffer-Wolff form.[18] The "low-energy" hybridization processes (associated with the single f-site occupancy—the conduction-band hybridization) are left intact (i.e., as in the original Anderson-lattice Hamiltonian) and yield the itineracy of the bare atomic f electrons. The crucial feature of Eq. (1) is thus the exclusion of f-site double occupancies, which effectively leads to the spin-dependent renormalization of the hybridization and in turn, to SDM, as well as to the virtual (f-c) hopping inducing real-space pairing, both within a single formal scheme. In the *Kondo-lattice limit* (i.e., when $n_f \equiv \langle \sum_\sigma N_{i\sigma}(1 - N_{i\bar\sigma})\rangle \equiv 1 - \delta$, with $\delta \ll 1$) and in the saddle-point or Gutzwiller approximations,[5,13] Hamiltonian (1) can be brought (up to a constant term) into an effective single-narrow-band form with the BCS type of pairing, which is (if we include also the Zeeman term—field $H \neq 0$)

$$\mathcal{H} = \sum_{\mathbf{k}\sigma} (q_\sigma \epsilon_{\mathbf{k}} - \sigma g \mu_B H - \mu) \psi_{\mathbf{k}\sigma}^\dagger \psi_{\mathbf{k}\sigma}$$
$$- \frac{1}{N} \sum_{\mathbf{kk'Q}} \frac{4 V_{\mathbf{k}}^2 V_{\mathbf{k'}}^2}{\epsilon_f^2 (\epsilon_f + U)} R_{\sigma\bar{\sigma}} \gamma_{\mathbf{k}} \gamma_{\mathbf{k'}} \psi_{\mathbf{k}\uparrow}^\dagger \psi_{-\mathbf{k}+\mathbf{Q}\downarrow}^\dagger \psi_{-\mathbf{k'}+\mathbf{Q}\downarrow} \psi_{\mathbf{k'}\uparrow}.$$

$$(3)$$

The above operators are those for the fermions in itinerant f states, i.e., $\psi_{\mathbf{k}\sigma}^\dagger \approx f_{\mathbf{k}\sigma}^\dagger$. The quantity $q_\sigma \epsilon_{\mathbf{k}}$ is the effective band energy of f electrons induced by the hybridization [cf. Fig. 1(c)], N is the number of sites, $\gamma_{\mathbf{k}}$ is a complicated function of quasimomentum $\mathbf{k}$ (cf. Appendix A), and $V_{\mathbf{kk'}} = -4 V_{\mathbf{k}}^2 V_{\mathbf{k'}}^2 / [\epsilon_f^2 (\epsilon_f + U)]$ is the strength of the pairing potential, taken in the following for the case of intra-atomic form of hybridization, $V_{\mathbf{k}} = V$. The factor q_σ, which in the $U \to \infty$ limit has the form $q_\sigma = (1-n)/(1-n_\sigma)$, with $n \approx n_f$, is the band renormalization factor leading to SDM, with $m_\sigma / m_0 = q_\sigma^{-1}$. Physically, the pairing results from the Kondo-type-induced f-magnetic moment self-screening of the heavy quasiparticles since they obey the Fermi-Dirac statistics. The renormalization factor of the pairing part $R_{\sigma\bar{\sigma}} \sim (q_\sigma q_{\bar{\sigma}})^{1/2}$ will be regarded here as a constant reducing only the pairing potential magnitude, i.e., $V_0 \equiv \frac{4 V^4}{\epsilon_f^2 (\epsilon_f + U)} R_{\sigma\bar{\sigma}}$. In what follows we take a simplified form of $\gamma_{\mathbf{k}}$ as of the d-wave symmetry, i.e., $\gamma_{\mathbf{k}} = \cos k_x - \cos k_y$. In general, the separable potential derived in Appendix A, $V_{\mathbf{kk'}} = g(\mathbf{k}) g(\mathbf{k'})$, should be expanded in terms of the $l=0$, $l=2$, etc., components and thus more complicated mixed s- and d-wave paired states are conceivable.

A few important physical remarks conveying principal features of our approach are in place here. First, the original atomic f electrons acquire itinerant (band) properties by a three-step process: hopping $f \to c$ from the atomic to the bare conduction-band (c) states followed by a propagation in the conduction band $(c \to c)$ and a subsequent deexcitation $c \to f$ [for illustration see Fig. 1(c)]. Hence, the bare f-f hopping amplitude is of the order $t \equiv (V/\epsilon_f)^2 t^{(c)}$, where $t^{(c)}$ is the hopping amplitude between the nearest-neighbor pair $\langle m, n \rangle$ in the conduction band. The processes leading simultaneously to both real-space pairing and itinerancy of f electrons are represented schematically in Figs. 1(a)–1(c). Second, as said above, the mechanism of pairing is of similar origin as that in t-J model, as discussed elsewhere.[17] In the present case it originates from the f-c virtual hopping, whereas in the latter case it is induced by the d-d virtual hopping. This means that the pairing here is also driven by the kinetic exchange, this time of the Kondo type. Third, the strongly correlated and hybridized electrons form an almost localized Fermi liquid of electrons in a single very narrow band of f states, when $\delta \ll 1$. The last assumption means that the number of quasiparticles is characterized by the band filling $n \approx n_f$ (related to, e.g., cerium valency by Ce^{+4-n_f}) and is regarded as constant as a function of T and H which is valid only at low temperature $T \ll T_K$ (T_K is the effective Kondo temperature cf. Karbowski and Spałek in Ref. 12). Finally, T_K plays the role of the f-electron bandwidth and its value is of the order $2z|t^{(c)}|(V/\epsilon_f)^2 (1-n)/(1-n/2) \approx 10^{-2} t^{(c)} \equiv 2z\tilde{t}$, where $\tilde{t}$ is an effective f-electron hopping (i.e., includes the double f occupancy exclusion. Since t is a

fraction of eV, then $\tilde{t} \simeq T_K$ is in the regime of the order 10 K (here it is about 5 K, see below). The extreme narrow bandwidth of the quasiparticle band explains why the heavy-electron systems are so sensitive to moderate applied fields on the order of 10 T; this is because the Zeeman energy may represent even a sizable portion of their Fermi energy. Note also that in this narrow-band regime we have assumed that the f-band filling n is fixed, i.e., independent of T and H. This is not true in the general Anderson-lattice case as, strictly speaking, only the total number of electrons $n_c + n_f = n$ is fixed.

One should mention that the present model differs from those representing either hybridized bands with multiple gaps[19] or that containing Kondo-type coupling introduced at the start,[20] as in this paper we introduce both heavy quasiparticles (with SDM) and the real-space Kondo-type pairing within a single framework. Additionally, as we introduce an effective single narrow f-band picture, only a single gap of intraband type emerges and is caused by the hybrid $(f$-$c)$ pairing. For simplicity, we neglect much smaller fourth-order f-f exchange interaction $\propto V^4 / U^3$ which also contributes to the pairing among the quasiparticles of f character in the Kondo-lattice limit.

B. Paired states: BCS vs FFLO

On the basis of the above discussion (cf. also Appendix A), the starting Hamiltonian for analyzing paired states is assumed of the form

$$\mathcal{H} = \sum_{\mathbf{k}\sigma} (\epsilon_{\mathbf{k}\sigma} - \sigma g \mu_B H - \mu) f_{\mathbf{k}\sigma}^\dagger f_{\mathbf{k}\sigma}$$
$$- \frac{V_0}{N} \sum_{\mathbf{kk'Q}} \gamma_{\mathbf{k}} \gamma_{\mathbf{k'}} f_{\mathbf{k}\uparrow}^\dagger f_{-\mathbf{k}+\mathbf{Q}\downarrow}^\dagger f_{-\mathbf{k'}+\mathbf{Q}\downarrow} f_{\mathbf{k'}\uparrow}. \quad (4)$$

Next, we introduce explicitly the quasiparticle states and analyze the relative stability of the BCS and the FFLO condensed states, the latter defined by the center-of-mass momentum $\mathbf{Q} \neq 0$ of the Cooper pairs. As mentioned already, we consider here the homogeneous FF type of FFLO phase, i.e., $\Delta(\mathbf{r}) = \Delta_{\mathbf{Q}} e^{i\mathbf{Qr}}$. Having in mind different gap symmetries, we assume that $\Delta_{\mathbf{k},\mathbf{Q}} \equiv \Delta_{\mathbf{Q}} \gamma_{\mathbf{k}}$, where the d-wave symmetry is expressed via $\gamma_{\mathbf{k}}$. We analyze explicitly the case of quasi-two-dimensional superconductor[21] in a clean limit, where Pauli-limiting situation[22] is well defined. Also, we introduce the dispersion relation in the itinerant f-electron quasiparticle band, which is parametrized as follows:

$$\epsilon_{\mathbf{k}\sigma} \equiv q_\sigma [-2t(\cos k_x + \cos k_y) + 4t' \cos k_x \cos k_y] \quad (5)$$

with t and t' being first two hopping integrals between the nearest and the next-nearest neighbors, respectively (in the numerical calculations we take $t'/t = 0.5$). This electronic structure represents main quasi-two-dimensional features of electronic states for both $CeCoIn_5$ and organic systems, in which FFLO has been discovered (cf. Singleton *et al.* and Cho *et al.* in Ref. 15), but SDM has not. Using the standard diagonalization techniques (cf. also Appendix B) we obtain the quasiparticle energies in the superconducting state in the form more general than that in Refs. 21 and 23, i.e.,

$$E_{\mathbf{k},\mathbf{Q},\alpha} = \frac{1}{2}(\epsilon_{\mathbf{k}\uparrow} - \epsilon_{-\mathbf{k}+\mathbf{Q}\downarrow}) - g\mu_B H + \alpha \frac{1}{2}[(\epsilon_{\mathbf{k}\uparrow} + \epsilon_{-\mathbf{k}+\mathbf{Q}\downarrow} - 2\mu)^2$$

$$+ 4|\Delta_{\mathbf{k},\mathbf{Q}}|^2]^{1/2}, \qquad (6)$$

where the sign $\alpha = +$ corresponds to the particle and the sign $\alpha = -$ to the hole excitations, respectively. In the above equation μ is the chemical potential and the gap function is determined for each phase separately from the self-consistent equation

$$\Delta_{\mathbf{Q}} = \frac{V_0 \Delta_{\mathbf{Q}}}{N} \sum_{\mathbf{k}} \gamma_{\mathbf{k}}^2 \frac{f(E_{\mathbf{k},\mathbf{Q}-}) - f(E_{\mathbf{k},\mathbf{Q}+})}{E_{\mathbf{k},\mathbf{Q}+} - E_{\mathbf{k},\mathbf{Q}-}}. \qquad (7)$$

This equation must be supplemented by the corresponding equations for μ and n_σ. Explicitly, spin-subband filling factors are determined from the conditions

$$n_\uparrow = \frac{1}{N} \sum_{\mathbf{k}} \frac{1}{E_{\mathbf{k},\mathbf{Q},+} - E_{\mathbf{k},\mathbf{Q},-}}$$

$$\times [(E_{\mathbf{k},\mathbf{Q},+} + \epsilon_{-\mathbf{k}+\mathbf{Q}\downarrow} - \mu - g\mu_B H)f(E_{\mathbf{k},\mathbf{Q},+})$$

$$- (E_{\mathbf{k},\mathbf{Q},-} + \epsilon_{-\mathbf{k}+\mathbf{Q}\downarrow} - \mu - g\mu_B H)f(E_{\mathbf{k},\mathbf{Q},-})], \qquad (8)$$

$$n_\downarrow = 1 - \frac{1}{N} \sum_{\mathbf{k}} \frac{1}{E_{\mathbf{k},\mathbf{Q},+} - E_{\mathbf{k},\mathbf{Q},-}}$$

$$\times [(E_{\mathbf{k},\mathbf{Q},+} + \epsilon_{\mathbf{k}\uparrow} - \mu - g\mu_B H)f(E_{\mathbf{k},\mathbf{Q},+})$$

$$- (E_{\mathbf{k},\mathbf{Q},-} + \epsilon_{\mathbf{k}\uparrow} - \mu - g\mu_B H)f(E_{\mathbf{k},\mathbf{Q},-})]. \qquad (9)$$

For a given $\mathbf{Q}$ Eqs. (7)–(9) form a self-consistent system for $\Delta_{\mathbf{Q}}$, n_σ, and μ. In practice, one has to find a value of $\mathbf{Q}$ that minimizes the free energy corresponding to the calculated $\Delta_{\mathbf{Q}}$, n_σ, and μ. The general free energy of the Landau type is given by

$$\mathcal{F} = -k_B T \sum_{\mathbf{k}} \sum_{\alpha=\pm} \ln[1 + \exp(-E_{\mathbf{k},\mathbf{Q},\alpha}/k_B T)] + \mu N n$$

$$+ \sum_{\mathbf{k}} (\epsilon_{-\mathbf{k}-\mathbf{Q}\downarrow} - \mu + g\mu_B H) + N|\Delta_{\mathbf{Q}}|^2/V_0. \qquad (10)$$

Since the problem is numerically complicated, we used two independent methods to be assured that the global minimum has been found, as well as to check for their relative accuracy: first, for each value of $\mathbf{Q}$ from a 160×160 grid in a quarter of the Brillouin zone, we solve the system of Eqs. (7)–(9) and choose that corresponding to the lowest value of $\mathcal{F}$. The sums in the equations were calculated directly using a grid of the same density, as for $\mathbf{Q}$. In the second method, we directly looked for a global minimum of $\mathcal{F}$ with respect to $\mathbf{Q}$, $\Delta_{\mathbf{Q}}$, and n_σ. The chemical potential was calculated from the condition for the total number of electrons, $n_\sigma + n_{\bar\sigma} = n$. In the latter method the sums were replaced by the integrals over momenta in the first Brillouin zone. The physical properties emerging from such a procedure are presented as a function of both H and T and discussed next.

III. RESULTS AND PHYSICAL DISCUSSION

A. Normal state

In Fig. 2(a) we display the field dependence of the mass enhancement in the normal state for band filling $n = 0.97$, i.e., close to the integer value. Note a strong temperature dependence associated with the corresponding reduction in the magnetization ($n_\uparrow - n_\downarrow$). Taking $t = 83$ K, we estimate $\tilde{t} = 5$ K, i.e., the regime of physical fields $H < 20$ T as limited by $g\mu_B H/t \lesssim 0.1$, where the mass splitting becomes indeed essential. In Fig. 2(b) we plot the field dependence of the quasiparticle density of states. One observes not only a Zeeman splitting of the spin subbands but also their relative distortion due to the presence of the band narrowing factor q_σ (note that here the spin $\sigma = +1$ subband is that representing the spin-majority band). The observed rapid change in the density of states with the increasing applied field influences essentially the relative stability of superconducting phases, as discussed next.

B. Superconducting states: Phase diagram

To characterize the relative stability of the BCS and the FFLO states, we plot the phase diagrams in Figs. 3(a) and 3(b) with the spin-independent masses (SIMs, taken as the average value $m_{av} = (m_\uparrow + m_\downarrow)/2$; then also $q_\sigma = q_{\bar\sigma} \equiv q$) and with SDM ($m_\sigma \neq m_{\bar\sigma}$), respectively. One notes an essential extension of the stability regime of the FFLO phase on the H-T plane in the latter case. This is the reason, we claim, why the FFLO state, most probably mixed with antiferromagnetism[16] has been observed in CeCoIn$_5$, where SDM were clearly established.[10] For the sake of completeness, we plot in Figs. 4(a) and 4(b) the values of the gap function $\Delta_{\mathbf{Q}}$ and the optimal center-of-mass momentum $\mathbf{Q}$, respectively ($\Delta_{\mathbf{k},\mathbf{Q}} \equiv \Delta_{\mathbf{k},\mathbf{Q}=0}$ in the BCS state). The gap amplitude $\Delta_{\mathbf{Q}}$ jumps across the BCS-FFLO border signaling the first-order transition. The transition to the normal phase seems to be continuous. The white dashed lines in Figs. 3(a) and 3(b) mark the critical field H_{c2} for the d-wave BCS state. Also, only if we include SDM, the uppermost critical field is spectacularly curved upward, what is observed in the organic systems (cf. Singleton *et al.* and Cho *et al.* in Ref. 15). However, one must mention that SDM have not been detected as yet in the latter system. One should note that the free-energy differences at the transition are on the order of $10^{-4}t \approx 10^{-2}$ K at most (see Fig. 4), what makes particularly intricate achieving the proper numerical accuracy when extracting the solutions of the self-consistent integral equations for $\Delta_{\mathbf{Q}}$, n_σ, and μ. This circumstance is also the reason behind the statement that within our numerical accuracy we cannot decisively state that the FFLO-normal-state phase transition is continuous. The last remark is illustrated in Figs. 5(a) and 5(b), where we plot the gap magnitude $\Delta_{\mathbf{Q}}$ on the H-T plane. In Fig. 5(b) we provide the value of $\mathbf{Q}$, which is not fixed in the FFLO regime ($Q_x = Q_y \approx 0.6 - 0.9$ in π/a units, where a is the lattice constant).

From Figs. 3–5 we can draw the following conclusions. First, in the situation with SDM, the FFLO state becomes stable in an extended regime of applied field and tempera-
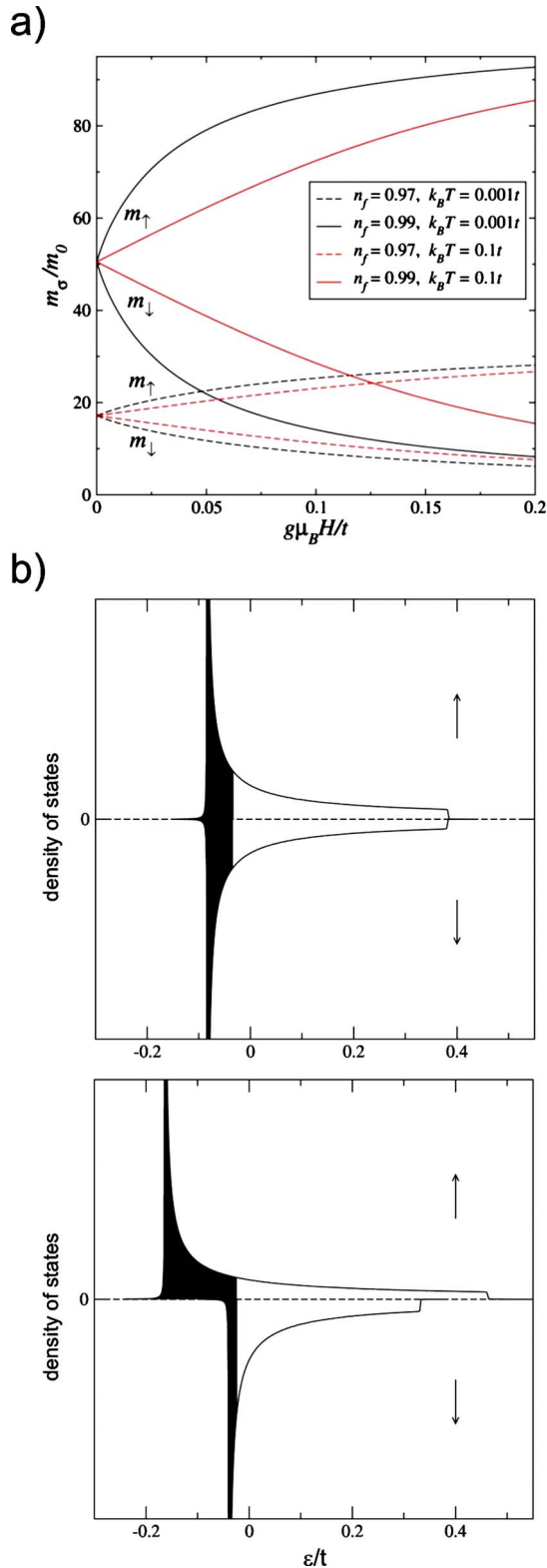
FIG. 2. (Color online) (a) Spin-dependent mass enhancement vs applied field H for selected values of both the filling n and temperature T specified. The effect is particularly strong for n very close to unity and for $T \ll T_K$. (b) Field dependence of the spin resolved density of quasiparticle states for $g\mu_B H/t = 0$ (middle graph) and 0.03 (lowest graph). Note that both the spin-subband relative distortion in an applied field and the Zeeman splitting is quite significant in the latter case.
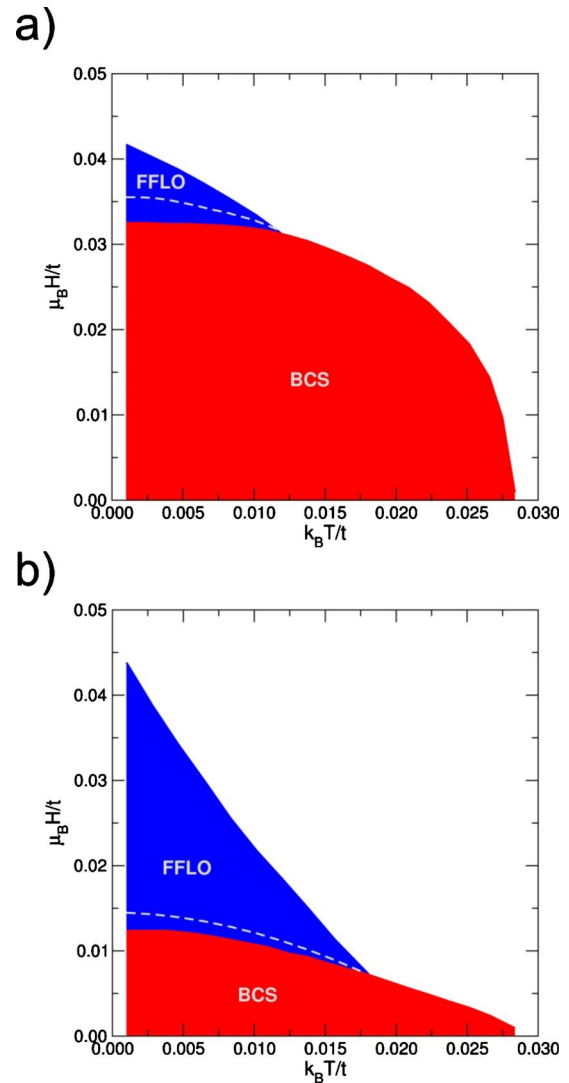
FIG. 3. (Color online) Phase boundaries for a two-dimensional d-wave superconductor with both (a) the SIMs and (b) the SDMs. The FFLO-BCS transition line is of discontinuous nature. The dashed line marks the stability limit of the BCS state as determined by the value of the second critical field H_{c2} for the BCS state. The values of parameters are $n = 0.97$ and $V_0 = 12.5$ K. For these values of the parameters, the superconducting transition temperature is $T_{sc} = 2.5$ K and the uppermost critical field for the FFLO phase is above 6 T. Note that the FFLO state is robust in the situation with SDM and this result is one of the principal features of the present paper.

ture. The reason for that is provided indirectly in Fig. 6, where we plot the exemplary curves of the relative magnetic polarization in the normal state, $(n_\uparrow - n_\downarrow)/(n_\uparrow + n_\downarrow)$, as a function of H. In the case with SDM, the magnetization grows at a slower pace vs H as compared to the situation with SIM. However, the spin resolved density of states [cf. Fig. 2(b)] is strongly distorted in an applied field causing the appearance of the FFLO state in relatively low applied fields. At the same time, the kinetic energy in the SDM case is lower than that in the SIM case since the spin-majority band broadens up with the increasing polarization. In effect, the formed FFLO state is stable in the wider interval of H. Second, if the
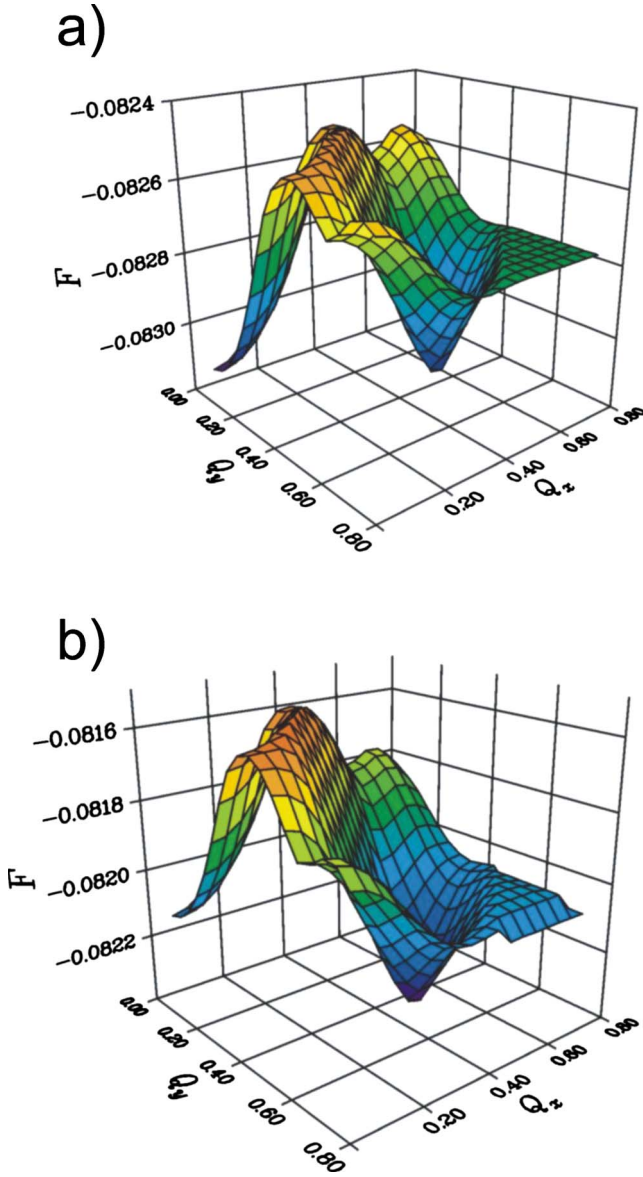
FIG. 4. (Color online) Exemplary free-energy shape contours (in units of t) on $\mathbf{Q} = (Q_x, Q_y)$ plane (in π/a units) for the BCS and FFLO states. The two separate minima $\mathbf{Q} = 0$ and $\mathbf{Q} \neq 0$ are the principal cause for a discontinuous switching from (a) BCS ($\mathbf{Q} = 0$) to (b) FFLO ($\mathbf{Q} \neq 0$) state.

FIG. 5. (Color online) Magnitude $\Delta_{\mathbf{Q}}$ of the superconducting gap function on the *H-T* plane (a) and the center-of-mass momentum components $Q_x = Q_y$ (b) for the same situation as in Fig. 3 and for the case with SDM. Only discontinuity of $\Delta_{\mathbf{Q}}$ matters in determining the order of the BCS→FFLO transition. Note also that the value of $\mathbf{Q}$ varies with changing *H* and *T* in the latter phase.

value of $t = 83$ K is taken, then the value of critical temperature for $H = 0$ is $T_{sc} \approx 0.03t \approx 2.5$ K. Parenthetically, the hopping magnitude for the quasiparticles is $\tilde{t} = tq = 5$ K. The uppermost critical field is then quite large (above $6T$), so indeed we have an example of high-field low-temperature unconventional superconducting state. For the sake of completeness, in Fig. 7 we compare the magnetization curves in the superconducting and the normal states (with a discontinuity at the BCS→FFLO boundary). The discontinuity demonstrates additionally the first-order nature of the transition. It is worth noting that the transition between the two spin-singlet superconducting phases induces a discontinuous metamagnetic transition even though the magnetization curve is continuous in the normal state. This characteristic

can thus provide an experimental indication for the nature of BCS-FFLO transition.

IV. CONCLUDING REMARKS

A. Outlook

Although the present results cannot be directly applied to the systems such as quasi-two-dimensional CeCoIn$_5$ or organic superconductors, they delineate principal nontrivial features of FFLO state in strongly correlated systems with *d*-wave form of the gap. Namely, from the results above it follows, that the SDMs play an important quantitative, if not
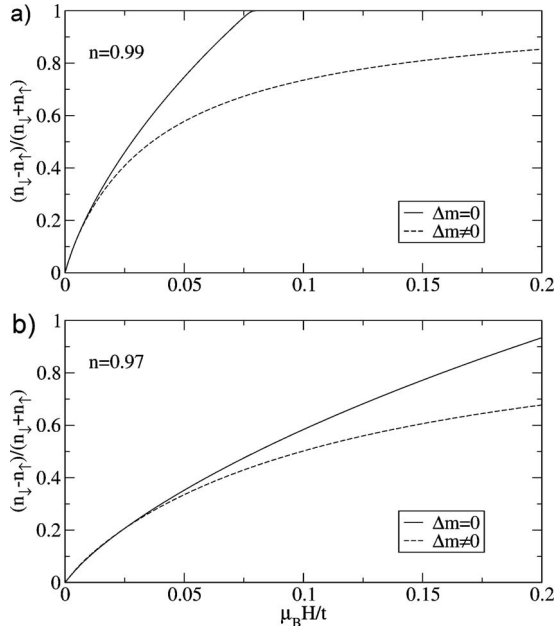
FIG. 6. Exemplary magnetization curves in the normal state for the two selected band fillings: (a) $n=0.99$ and (b) $n=0.97$. The system magnetizes less rapidly in the case with SDM ($\Delta m \neq 0$). However, in that case the spin resolved density of states is strongly influenced in the applied field [cf. Fig. 2(b)] and this last factor determines directly the changes in the SDM case.

crucial role, in extending the (H,T) regime of the FFLO phase stability and therefore should be taken into account in realistic models of superconductivity in heavy-fermion compounds. The spin-split masses appear in both the Gutzwiller (or mean field) and other approaches,[8,9] so they represent an essential ingredient of the theory of correlated states in magnetically polarized state.
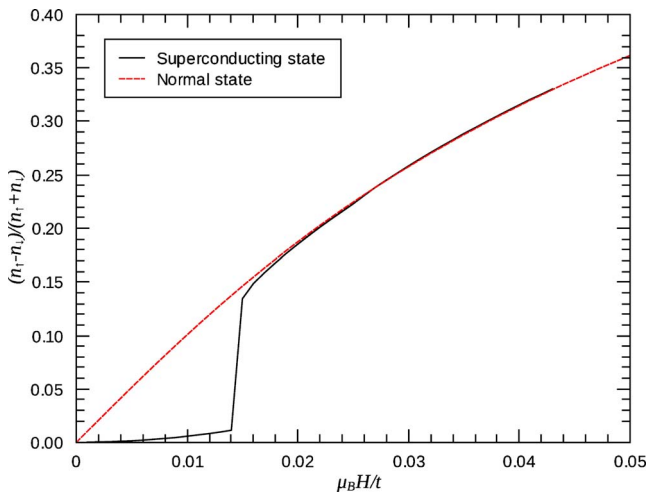
FIG. 7. (Color online) Magnetization curves in the superconducting (continuous line) and the normal states (dashed line). The parameters are $n=0.97$ and $V_0=12.5$ K. Note that the transition between the superconducting states is associated with a metamagnetic transition followed by a continuous evolution to the normal state.

One has to note that in the FFLO phase there are substantial unpaired regions in the Brillouin zone in which either $E_{\mathbf{k},\mathbf{Q},+}<0$ or $E_{\mathbf{k},\mathbf{Q},-}>0$. The unpaired regions can easily become magnetic and hence the antiferromagnetism-FFLO coexistence must be analyzed with care. This is particularly so since the real-space pairing discussed here is induced by an antiferromagnetic type of kinetic exchange. The coexistence of superconductivity with antiferromagnetism has not been tackled in this work since the primary purpose here is to demonstrate the intrinsic relevance of the spin dependence of the quasiparticle mass on the FFLO stability and other physical properties.

In brief, while our mean-field calculations including the nonstandard nature of quasiparticles, but without antiferromagnetism, cannot be regarded as applicable directly to systems such as CeCoIn$_5$, they provide a strong indication concerning the possible physics of the FFLO appearance in strongly correlated systems.

B. Comparison with the electron-gas case

The present paper extends the earlier works for the correlated electron gas in both three[24] and two[25] spatial dimensions. The results here differ in a number of respects from those presented earlier, both in SDM (Ref. 25) and SIM (Ref. 26) situations. First, in the present model there is only one stable FFLO phase with $Q_x=Q_y$ (such result has also been obtained in Ref. 27 in the SIM case), whereas for a 2D gas with d-wave gap symmetry also the phase with $\mathbf{Q}=(Q_x,0)$ is stable for magnetic fields close to H_{c2} and at low temperature[25,26] (both in the SDM and SIM cases). Second, here the center-of-mass momentum magnitude is of the order $Q \approx \pi/a$, that is, about an order of magnitude larger than that for the gas case (for which $Q \approx 0.05k_F$). Third, the critical field H_{c2} in the present model is almost the same for SDM and SIM cases, whereas for the electron-gas model the critical field for SDM case is about four times higher than that for the corresponding SIM case. Fourth, the FFLO phase benefits energetically to a greater extent from SDM in the present model than for the gas [i.e., it occupies a larger portion of the phase diagram on (H,T) plane]. Fifth, the BCS-FFLO transition in the present situation with SDM is always discontinuous and is associated with a large jump of magnetization (cf. Fig. 7). In the gas case this transition is of the first order only for $T \lesssim 0.8$ K, and both the magnetization and the gap jumps at the BCS-FFLO boundary are much smaller. Finally, the BCS-FFLO transition line here descends with the increasing T (see Fig. 3), whereas for the gas model this line ascends with the increasing T and resembles the experimental findings.[15] The differences are caused mainly by the circumstance that only in the present case van Hove singularity appears explicitly. There are also other qualitative differences in the character and shape of the density of states [cf. Figs. 2(b) and 2(c)]. These differences induce quite large mass splitting $\Delta m \equiv m_{\downarrow}-m_{\uparrow}$ in the present situation ($\Delta m/m_{\uparrow}$ is almost 100% in the field $H \approx H_{c2}$) whereas it is small ($\Delta m/m_{\uparrow} \approx 10\%$) in the corresponding gas case.

However, there is one additional difference between the approach of Ref. 25 and that presented here. Namely, in the

former case[24,25] we include also the effective field h_{cor} coming from correlations and obtained, e.g., in the saddle-point solution of the slave-boson approach. Such an effective self-consistent field[28] does not appear in the standard Gutzwiller approximation and in the limit of no double occupancies ($d = 0$) for a tight-binding model would lead to ferromagnetism close to the integer band filling. Therefore, we decided not to include this feature of the correlated states (i.e., going beyond the Gutzwiller approach) until a full phase diagram, incorporating also antiferromagnetic or spin-density-wave states, is constructed.

APPENDIX A: FROM KONDO COUPLING TO REAL-SPACE PAIRING IN AN ALMOST LOCALIZED FERMI LIQUID OF HEAVY QUASIPARTICLES

Even though the real-space hybrid pairing has been discussed earlier,[12] we summarize here its main features to demonstrate its difference with the spin-fluctuation type of pairing mechanism.[29] This pairing mechanism is not as widely known as the spin-fluctuation pairing. At the beginning we should note that as the real-space pairing involves all correlated particles, the chemical potential must be self-consistently adjusted in each of the phases considered.

We start from the Anderson Hamiltonian

$$H = \sum_{mn\sigma} t_{mn} c_{m\sigma}^\dagger c_{n\sigma} + \epsilon_f \sum_{i\sigma} N_{i\sigma} + U \sum_i N_{i\uparrow} N_{i\downarrow}$$
$$+ \sum_{im\sigma} V_{im}(f_{i\sigma}^\dagger c_{m\sigma} + c_{m\sigma}^\dagger f_{i\sigma}) - \mu \left(\sum_{i\sigma} N_{i\sigma} + \sum_{m\sigma} n_{m\sigma} \right)$$
$$\tag{A1}$$

with $N_{i\sigma} \equiv f_{i\sigma}^\dagger f_{i\sigma}$. All other symbols and terms are explained in main text and in Ref. 12. The Hamiltonian is written in the position (real-space) representation, as we are going to discuss fermionic correlations in that language since the f-f intra-atomic interaction $\propto U$ constitutes the largest energy scale for this strongly correlated system.

The principal step involves the division of the f-c hybridization into two parts according to the prescription

$$f_{i\sigma}^\dagger c_{m\sigma} \equiv (1 - N_{i\bar\sigma} + N_{i\bar\sigma}) f_{i\sigma}^\dagger c_{m\sigma}$$
$$= (1 - N_{i\bar\sigma}) f_{i\sigma}^\dagger c_{m\sigma} + N_{i\bar\sigma} f_{i\sigma}^\dagger c_{m\sigma}. \tag{A2}$$

The first term represents the hybridization (hopping) processes between the subsystems with no double occupancy of the f state involved, whereas the second contains the hopping induced by hybridization with formation of the double f-site occupancy or the reverse process. The situation is shown schematically in Fig. 8. Since $|\epsilon_f - \mu| \ll \epsilon_f - \mu + U$, the processes (I) are those at low energy (real f-c mixing of states), whereas the processes (II) are those realized only as virtual
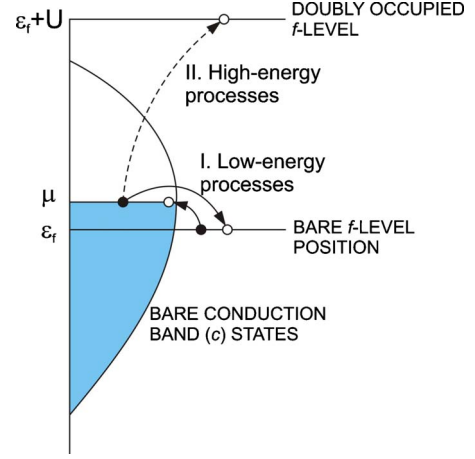
FIG. 8. (Color online) Schematic representation of hybridization (c-f mixing) processes as f-occupation-dependent hopping processes and their division into low- and high-energy processes. The former (I) lead to the formation of hybridized heavy-quasiparticle states; the other (II) lead to the Kondo-type coupling which in turn is expressed as real-space (hybrid) pairing in the second order in $V/(U + \epsilon_f)$.

processes and are accounted for in the second order in $V/(\epsilon_f + U)$. In this manner, our canonical transformation of deriving the effective Hamiltonian[12] differs from the standard Schrieffer-Wolff transformation[18] since only the process (II) yields the effective coupling. Performing canonical transformation replacing the process (II) in the first order we obtain the effective Hamiltonian in the form

$$H = \sum_{mn\sigma} \left(t_{mn} + \sum_i V_{mi} V_{in} \frac{\nu_{i\bar\sigma}}{\epsilon_f + U} \right) c_{m\sigma}^\dagger c_{n\sigma} + \epsilon_f \sum_i \nu_{i\sigma}$$
$$+ \sum_{im\sigma} V_{im}(1 - N_{i\bar\sigma})(f_{i\sigma}^\dagger c_{m\sigma} + c_{m\sigma}^\dagger f_{i\sigma})$$
$$+ \sum_{im} \frac{2 V_{im}^2}{\epsilon_f + U} \left(\mathbf{S}_i \cdot \mathbf{s}_m - \frac{1}{4} \nu_i n_m \right)$$
$$+ \frac{1}{\epsilon_f + U} \sum_{imn\sigma} V_{mi} V_{in} S_i^\sigma c_{m\bar\sigma}^\dagger c_{n\sigma}, \tag{A3}$$

where $t_{mn} \equiv t_{mn} - \mu \delta_{mn}$ and $\epsilon_f \equiv \epsilon_f - \mu$. Also, in this Hamiltonian we have projected out completely the double occupancies, as well as have defined the quantities for f electrons: $\nu_{i\sigma} \equiv N_{i\sigma}(1 - N_{i\bar\sigma})$, $\nu_i \equiv \Sigma_\sigma \nu_{i\sigma}$, $\mathbf{S}_i \equiv (S_i^\sigma, S_i^z) = [f_{i\sigma}^\dagger f_{i\bar\sigma}, \frac{1}{2}(\nu_{i\uparrow} - \nu_{i\downarrow})]$, and the corresponding quantities for conduction-band electrons: $n_{m\sigma} \equiv c_{m\sigma}^\dagger c_{m\sigma}$, $n_m \equiv \Sigma_\sigma n_{m\sigma}$, and $\mathbf{s}_m \equiv (s_m^\sigma, s_m^z) = [c_{m\sigma}^\dagger c_{m\bar\sigma}, \frac{1}{2}(n_{m\uparrow} - n_{m\downarrow})]$. We see that the third and the fourth terms in Eq. (A3) represent the truncated f-c mixing and the Kondo coupling, respectively. Ignoring the higher order part in the first term and introducing the hybrid pairing operators [Eq. (2)] in the strongly correlated state, we arrive at Hamiltonian (1) which can also be represented in the form

$$\mathcal{H} \equiv P_G H P_G = P_G \left[\sum_{mn\sigma} t_{mn} c_{m\sigma}^\dagger c_{n\sigma} + \epsilon_f \sum_{i\sigma} N_{i\sigma} \right.$$

$$\left. + \sum_{im\sigma} V_{im} (f_{i\sigma}^\dagger c_{m\sigma} + c_{m\sigma}^\dagger f_{i\sigma}) - 2 \sum_{imn} \frac{V_{im} V_{in}}{\epsilon_f + U} A_{im}^\dagger A_{in} \right] P_G,$$

$$(A4)$$

where $P_G = \Pi_i (1 - N_{i\uparrow} N_{i\downarrow})$ is the Gutzwiller projection operator and

$$A_{im}^\dagger = \frac{1}{\sqrt{2}} (f_{i\uparrow}^\dagger c_{m\downarrow}^\dagger - f_{i\downarrow}^\dagger c_{m\uparrow}^\dagger); \quad A_{im} = (A_{im}^\dagger)^\dagger. \quad (A5)$$

The system described by either Hamiltonian (A3) or (A4) does not represent a Fermi liquid. This is illustrated by, e.g., nonfermionic commutation relations between the projected operators $\widetilde{f}_{i\sigma} \equiv f_{i\sigma} (1 - N_{i\bar{\sigma}})$ and $\widetilde{f}_{i\sigma}^\dagger \equiv f_{i\sigma}^\dagger (1 - N_{i\bar{\sigma}})$,

$$\{\widetilde{f}_{i\sigma}, \widetilde{f}_{j\sigma'}^\dagger\} = \delta_{ij} [(1 - N_{i\bar{\sigma}}) \delta_{\sigma\sigma'} + S_i^{-\sigma} (1 - \delta_{\sigma\sigma'})]. \quad (A6)$$

However, at this stage the canonical approximation is of Gutzwiller type[13] and yields the effective Hamiltonian

$$\mathcal{H} = \sum_{mn\sigma} t_{mn} c_{m\sigma}^\dagger c_{n\sigma} + \sum_{i\sigma} \widetilde{\epsilon}_f N_{i\sigma} + \sum_{im\sigma} \widetilde{V}_{im\sigma} (f_{i\sigma}^\dagger c_{m\sigma} + c_{m\sigma}^\dagger f_{i\sigma})$$

$$- 2 \sum_{imn} \frac{V_{im} V_{in}}{\epsilon_f + u} R_{\sigma\bar{\sigma}} A_{im}^\dagger A_{in}. \quad (A7)$$

Strictly speaking, this type of renormalization of not only V_{im} but also ϵ_f and the pairing potential $R_{\sigma\bar{\sigma}}$ follows from the slave-boson formulation which generalizes the standard Gutzwiller approximation. In the above expression $\widetilde{V}_{im\sigma} = V_{im} q_\sigma$, where q_σ is the Gutzwiller renormalization factor[13]

$$q_\sigma(d^2) = \frac{1}{n_{f\sigma}(1 - n_{f\sigma})} \{(n_{f\sigma} - d^2)(1 - n_f + d^2) + (n_{f\bar{\sigma}} - d^2)d^2$$

$$+ 2[(n_{f\sigma} - d^2)(n_{f\bar{\sigma}} - d^2)d^2(1 - n_f + d^2)]^{1/2}\}. \quad (A8)$$

For simplicity, one takes $\widetilde{\epsilon}_f$ and $R_{\sigma\bar{\sigma}}$ as constants. A methodological remark is in place here. Namely, by introducing back original (not projected) operators $f_{i\sigma}$ (and $f_{i\sigma}^\dagger$) and A_{im} ($A_{im}^\dagger$) we transform the Hamiltonian to that representing an *almost localized Fermi liquid* if $n_f = 1 - \delta$, $\delta \ll 1$. Hamiltonian (A7) can be transformed to the momentum representation in which it takes the form

$$\mathcal{H} = \sum_{\mathbf{k}\sigma} [\epsilon_{\mathbf{k}\sigma} c_{\mathbf{k}\sigma}^\dagger c_{\mathbf{k}\sigma} + \widetilde{\epsilon}_{f\sigma} f_{\mathbf{k}\sigma}^\dagger f_{\mathbf{k}\sigma} + \widetilde{V}_{\mathbf{k}\sigma} f_{\mathbf{k}\sigma}^\dagger c_{\mathbf{k}\sigma} + \widetilde{V}_{\mathbf{k}\sigma}^* c_{\mathbf{k}\sigma}^\dagger f_{\mathbf{k}\sigma}]$$

$$- \frac{2}{\epsilon_f + U} \frac{1}{N} \sum_{\mathbf{k}\mathbf{k}'\mathbf{Q}} V_{\mathbf{k}} V_{\mathbf{k}'}^* A_{\mathbf{k},\mathbf{Q}}^\dagger A_{\mathbf{k}',\mathbf{Q}} \quad (A9)$$

with

$$A_{\mathbf{k}\mathbf{Q}}^\dagger = \frac{1}{\sqrt{2}} (f_{\mathbf{k}+\mathbf{Q}/2\uparrow}^\dagger c_{-\mathbf{k}+\mathbf{Q}/2\downarrow}^\dagger - f_{-\mathbf{k}+\mathbf{Q}/2\downarrow}^\dagger c_{\mathbf{k}+\mathbf{Q}/2\uparrow}^\dagger). \quad (A10)$$

The single-particle part can be easily diagonalized by moving to the hybridized basis, whereas the pairing part is represented by a *separable* pairing potential. We shall proceed

with the transformation to the hybridized basis first, which yields the following transformed pairing part for the lower hybridized band:

$$\mathcal{H} = \sum_{\mathbf{k}\sigma} E_{\mathbf{k}\sigma} \alpha_{\mathbf{k}\sigma}^\dagger \alpha_{\mathbf{k}\sigma} - \frac{4}{\epsilon_f + U}$$

$$\times \sum_{\mathbf{k}\mathbf{k}'\mathbf{Q}} \frac{|V_{\mathbf{k}} V_{\mathbf{k}'}|^2 (q_\sigma q_{\bar{\sigma}})^{1/2}}{[(\epsilon_{\mathbf{k}\sigma} - \widetilde{\epsilon}_{f\sigma})^2 + |\widetilde{V}_{\mathbf{k}\sigma}|^2]^{1/2} [(\epsilon_{\mathbf{k}'\bar{\sigma}} - \widetilde{\epsilon}_{f\bar{\sigma}})^2 + |\widetilde{V}_{\mathbf{k}'\bar{\sigma}}|^2]^{1/2}}$$

$$\times \alpha_{\mathbf{k}+\mathbf{Q}/2\uparrow}^\dagger \alpha_{-\mathbf{k}+\mathbf{Q}/2\downarrow}^\dagger \alpha_{-\mathbf{k}'+\mathbf{Q}/2\downarrow} \alpha_{\mathbf{k}'+\mathbf{Q}/2\uparrow} \quad (A11)$$

with

$$E_{\mathbf{k}\sigma} \equiv \frac{\epsilon_{\mathbf{k}\sigma} + \widetilde{\epsilon}_{f\sigma}}{2} - \left[\left(\frac{\epsilon_{\mathbf{k}\sigma} + \widetilde{\epsilon}_{f\sigma}}{2} \right)^2 + |\widetilde{V}_{\mathbf{k}\sigma}|^2 \right]^{1/2}. \quad (A12)$$

Note that in Eqs. (A11) and (A12) we have written the formulas for the spin-polarized situation. Also, the present form with $\mathbf{Q}/2$ momenta associated with the pairing part is equivalent with form (4) used in main text. For real $V_{\mathbf{k}}$, the hybridized basis reads $\alpha_{\mathbf{k}\sigma} = \cos \theta_{\mathbf{k}\sigma} f_{\mathbf{k}\sigma} + \sin \theta_{\mathbf{k}\sigma} c_{\mathbf{k}\sigma}$, with the condition

$$\tan 2\theta_{\mathbf{k}\sigma} = \frac{2\widetilde{V}_{\mathbf{k}\sigma}}{\epsilon_{\mathbf{k}\sigma} - \widetilde{\epsilon}_{f\sigma}}. \quad (A13)$$

Taking the states on the Fermi surface we have $\tan 2\theta_{\mathbf{k}\sigma} \approx 2\theta_{\mathbf{k}\sigma}$, and hence $\theta_{\mathbf{k}\sigma} = \widetilde{V}_{\mathbf{k}\sigma} / \widetilde{\epsilon}_{f\sigma}$. In effect, $\alpha_{\mathbf{k}\sigma} \simeq f_{\mathbf{k}\sigma}$. The last estimate provides us with the starting Hamiltonian (4) in the single-band limit. The complicated $\mathbf{k}$ dependence of the pairing potential means that in general, the nature of the superconducting gap may take a form more complicated than pure extended s-wave or d-wave forms. Note also that even though the pairing potential contains explicitly the spin quantum numbers, it is in fact spin independent, as assumed in the main text.

APPENDIX B: BOGOLYUBOV-VALATIN-DE GENNES-NAMBU REPRESENTATION FOR THE CASE WITH SPIN-DEPENDENT MASSES

The whole procedure of diagonalizing Hamiltonian (4) is quite standard, as it can be brought up to the form

$$\mathcal{H} = \sum_{\mathbf{k}\sigma} (\epsilon_{\mathbf{k}\sigma} - \mu) f_{\mathbf{k}\sigma}^\dagger f_{\mathbf{k}\sigma} - g\mu_B H \sum_{\mathbf{k}} (f_{\mathbf{k}\uparrow}^\dagger f_{\mathbf{k}\uparrow} - f_{\mathbf{k}\downarrow}^\dagger f_{\mathbf{k}\downarrow})$$

$$+ \sum_{\mathbf{k}} (\Delta_{\mathbf{k}\mathbf{Q}}^* f_{\mathbf{k}\uparrow} f_{-\mathbf{k}+\mathbf{Q}\downarrow} + h.c.) + N \frac{\Delta_{\mathbf{Q}}^2}{V_0} \quad (B1)$$

with

$$\epsilon_{\mathbf{k}\sigma} \equiv q_\sigma [-2t (\cos k_x + \cos k_y) + 4t' \cos k_x \cos k_y],$$

$$(B2)$$

$$\Delta_{\mathbf{k},\mathbf{Q}} = -\frac{V_0}{N} \sum_{\mathbf{k}'} \gamma_{\mathbf{k}} \gamma_{\mathbf{k}'} \langle f_{-\mathbf{k}'+\mathbf{Q}\downarrow} f_{\mathbf{k}'\uparrow} \rangle. \quad (B3)$$

Equivalently, it can be cast in the Nambu 2×2 matrix form

$$\mathcal{H} = \sum_{\mathbf{k}} (f_{\mathbf{k}\uparrow}^{\dagger}, f_{-\mathbf{k}+\mathbf{Q}\downarrow})$$

$$\times \begin{pmatrix} \epsilon_{\mathbf{k}\uparrow} - g\mu_B H - \mu & \Delta_{\mathbf{k},\mathbf{Q}} \\ \Delta_{\mathbf{k},\mathbf{Q}}^{*} & -\epsilon_{-\mathbf{k}+\mathbf{Q}\downarrow} - g\mu_B H + \mu \end{pmatrix} \begin{pmatrix} f_{\mathbf{k}\uparrow} \\ f_{-\mathbf{k}+\mathbf{Q}\downarrow}^{\dagger} \end{pmatrix}$$

$$+ \sum_{\mathbf{k}} (\epsilon_{\mathbf{k}\downarrow} + g\mu_B H - \mu) + N\frac{\Delta_{\mathbf{Q}}^2}{V_0}. \tag{B4}$$

The eigenvalues $\lambda \equiv E_{\mathbf{k},\mathbf{Q},\pm}$ of this Hamiltonian are calculated readily from the determinant involving the above 2×2 matrix, i.e., from the equation

$$\det\begin{pmatrix} \epsilon_{\mathbf{k}\uparrow} - g\mu_B H - \mu - \lambda & \Delta_{\mathbf{k},\mathbf{Q}} \\ \Delta_{\mathbf{k},\mathbf{Q}}^{*} & -\epsilon_{-\mathbf{k}+\mathbf{Q}\downarrow} - g\mu_B H + \mu - \lambda \end{pmatrix} = 0 \tag{B5}$$

and they are given by

$$\lambda \equiv E_{\mathbf{k},\mathbf{Q},\pm} = \frac{1}{2}(\epsilon_{\mathbf{k}\uparrow} - \epsilon_{-\mathbf{k}+\mathbf{Q}\downarrow}) - g\mu_B H$$

$$\pm \frac{1}{2}[(\epsilon_{\mathbf{k}\uparrow} + \epsilon_{-\mathbf{k}+\mathbf{Q}\downarrow} - 2\mu)^2 + 4|\Delta_{\mathbf{k},\mathbf{Q}}|^2]^{1/2}. \tag{B6}$$

Note that we take the Zeeman energy in the form $[-g\mu_B H \Sigma_{\mathbf{k}}(n_{\mathbf{k}\uparrow} - n_{\mathbf{k}\downarrow})]$ so the state with magnetic moment $\sigma = \uparrow$ represents the spin-majority band. The Bogolyubov co-

herence factors $u_{\mathbf{k}}$ and $v_{\mathbf{k}}$ are determined from the set of linear homogeneous equations

$$\begin{pmatrix} \epsilon_{\mathbf{k}\uparrow} - g\mu_B H - \mu - \lambda & \Delta_{\mathbf{k},\mathbf{Q}} \\ \Delta_{\mathbf{k},\mathbf{Q}}^{*} & -\epsilon_{-\mathbf{k}+\mathbf{Q}\downarrow} - g\mu_B H + \mu - \lambda \end{pmatrix} \begin{pmatrix} u_{\mathbf{k}} \\ v_{\mathbf{k}} \end{pmatrix} = 0, \tag{B7}$$

together with the renormalization condition $|u_{\mathbf{k}}|^2 + |v_{\mathbf{k}}|^2 = 1$. Those factors determine the quasiparticle operators $\alpha_{\mathbf{k}}$ and $\beta_{\mathbf{k}}^{\dagger}$ corresponding to the eigenvalues $E_{\mathbf{k},\mathbf{Q},+}$ and $E_{\mathbf{k},\mathbf{Q},-}$, respectively, in the manner

$$\begin{pmatrix} \alpha_{\mathbf{k}} \\ \beta_{\mathbf{k}}^{\dagger} \end{pmatrix} = \begin{pmatrix} u_{\mathbf{k}} & v_{\mathbf{k}} \\ -v_{\mathbf{k}} & u_{\mathbf{k}} \end{pmatrix} \begin{pmatrix} f_{\mathbf{k}\uparrow} \\ f_{-\mathbf{k}+\mathbf{Q}\downarrow}^{\dagger} \end{pmatrix}. \tag{B8}$$

Explicitly, the Bogolyubov coherence factors are given by

$$u_{\mathbf{k}} = \left[\frac{1}{2}\left(1 + \frac{\epsilon_{\mathbf{k}\uparrow} + \epsilon_{-\mathbf{k}+\mathbf{Q}\downarrow} - 2\mu}{\sqrt{(\epsilon_{\mathbf{k}\uparrow} + \epsilon_{-\mathbf{k}+\mathbf{Q}\downarrow} - 2\mu)^2 + 4\Delta_{\mathbf{k},\mathbf{Q}}^2}}\right)\right]^{1/2}, \tag{B9}$$

$$v_{\mathbf{k}} = \left[\frac{1}{2}\left(1 - \frac{\epsilon_{\mathbf{k}\uparrow} + \epsilon_{-\mathbf{k}+\mathbf{Q}\downarrow} - 2\mu}{\sqrt{(\epsilon_{\mathbf{k}\uparrow} + \epsilon_{-\mathbf{k}+\mathbf{Q}\downarrow} - 2\mu)^2 + 4\Delta_{\mathbf{k},\mathbf{Q}}^2}}\right)\right]^{1/2}. \tag{B10}$$

Obviously, in the limit $H=0$, $\mathbf{Q}=0$ the expressions for λ, $u_{\mathbf{k}}$, and $v_{\mathbf{k}}$ reduce to the standard expressions from the BCS theory.

---

*maciek@phys.us.edu.pl

†ufspalek@if.uj.edu.pl

[1] E. Bauer, G. Hilscher, H. Michor, C. Paul, E. W. Scheidt, A. Gribanov, Y. Seropegin, H. Noël, M. Sigrist, and P. Rogl, Phys. Rev. Lett. **92**, 027003 (2004).

[2] G. Luke *et al.*, Nature (London) **394**, 558 (1998); for review see, Y. Maeno, T. M. Rice, and M. Sigrist, Phys. Today **54**(1), 42 (2001).

[3] H. Shimahara, Phys. Rev. B **62**, 3524 (2000).

[4] P. S. Riseborough, G. M. Schmiedeshoff, and J. L. Smith, in *The Physics of Superconductors*, edited by K. H. Bennemann and J. B. Ketterson (Springer-Verlag, Berlin, 2004) Vol. II, p. 889; Y. Matsuda and H. Shimahara, J. Phys. Soc. Jpn. **76**, 051005 (2007).

[5] J. Spałek, J. Solid State Chem. **88**, 70 (1990); M. Imada, A. Fujimori, and Y. Tokura, Rev. Mod. Phys. **70**, 1039 (1998); for Anderson lattice see, e.g., D. M. Newns and N. Read, Adv. Phys. **36**, 799 (1987); P. A. Lee, T. M. Rice, J. W. Serene, L. J. Sham, and J. W. Wilkins, Comments Condens. Matter Phys. **12**, 99 (1986).

[6] G. R. Stewart, Rev. Mod. Phys. **78**, 743 (2006), and references therein.

[7] P. A. Lee, N. Nagaosa, and X.-G. Wen, Rev. Mod. Phys. **78**, 17 (2006).

[8] J. Spałek and P. Gopalan, Phys. Rev. Lett. **64**, 2823 (1990); P. Korbel, J. Spałek, W. Wójcik, and M. Acquarone, Phys. Rev. B **52**, R2213 (1995); J. Bauer, Eur. Phys. J. B **68**, 201 (2009); R. Citro, A. Romano, and J. Spałek, Physica B **259-261**, 213 (1999); for recent review see, J. Spałek, *ibid.* **378-380**, 654 (2006); J. Spałek, Phys. Status Solidi B **243**, 78 (2006).

[9] S. Onari, H. Kontani, and Y. Tanaka, J. Phys. Soc. Jpn. **77**, 023703 (2008); J. Bauer and A. C. Hewson, Phys. Rev. B **76**, 035118 (2007).

[10] A. McCollam, S. R. Julian, P. M. C. Rourke, D. Aoki, and J. Flouquet, Phys. Rev. Lett. **94**, 186401 (2005).

[11] I. Sheikin, A. Gröger, S. Raymond, D. Jaccard, D. Aoki, H. Harima, and J. Flouquet, Phys. Rev. B **67**, 094420 (2003); M. Takashita, H. Aoki, T. Terashima, S. Uji, K. Maezawa, R. Settai, and Y. Onuki, J. Phys. Soc. Jpn. **65**, 515 (1996).

[12] J. Spałek, Phys. Rev. B **38**, 208 (1988); J. Spałek and P. Gopalan, J. Phys. (France) **50**, 2869 (1989); J. Karbowski and J. Spałek, Phys. Rev. B **49**, 1454 (1994); J. Spałek, *Encyclopedia of Physical Science and Technology*, 3rd ed. (Academic Press, San Diego, 2002), Vol. 16, pp. 251–289.

[13] T. M. Rice and K. Ueda, Phys. Rev. B **34**, 6420 (1986); C. M. Varma, W. Weber, and L. J. Randall, *ibid.* **33**, 1015 (1986); B. H. Brandow, *ibid.* **33**, 215 (1986).

[14] Z. J. Ying, M. Cuoco, C. Noce, and H. Q. Zhou, Phys. Rev. B **78**, 104523 (2008).

[15] C. Petrovic, P. G. Pagliuso, M. F. Hundley, R. Movshovich, J. L. Sarrao, J. D. Thompson, Z. Fisk, and P. Monthoux, J. Phys.: Condens. Matter **13**, L337 (2001); A. Bianchi, R. Movshovich,

C. Capan, P. G. Pagliuso, and J. L. Sarrao, Phys. Rev. Lett. **91**, 187004 (2003); K. Kakuyanagi, M. Saitoh, K. Kumagai, S. Takashima, M. Nohara, H. Takagi, and Y. Matsuda, *ibid.* **94**, 047602 (2005); C. F. Miclea, M. Nicklas, D. Parker, K. Maki, J. L. Sarrao, J. D. Thompson, G. Sparn, and F. Steglich, *ibid.* **96**, 117001 (2006); J. Singleton, J. A. Symington, M.-S. Nam, A. Ardavan, M. Kurmoo, and P. Day, J. Phys.: Condens. Matter **12**, L641 (2000); R. Lortz, Y. Wang, A. Demuer, P. H. M. Böttger, B. Bergk, G. Zwicknagl, Y. Nakazawa, and J. Wosnitza, Phys. Rev. Lett. **99**, 187002 (2007); K. Cho, B. E. Smith, W. A. Coniglio, L. E. Winter, C. C. Agosta, and J. A. Schlueter, Phys. Rev. B **79**, 220507(R) (2009).

[16] G. Koutroulakis, M. D. Stewart, Jr., V. F. Mitrović, M. Horvatić, C. Berthier, G. Lapertot, and J. Flouquet, Phys. Rev. Lett. **104**, 087001 (2010); M. Kenzelmann, Th. Strässle, C. Niedermayer, M. Sigrist, B. Padmanabhan, M. Zolliker, A. D. Bianchi, R. Movshovich, E. D. Bauer, J. L. Sarrao, and J. D. Thompson, Science **321**, 1652 (2008); B.-L. Young, R. R. Urbano, N. J. Curro, J. D. Thompson, J. L. Sarrao, A. B. Vorontsov, and M. J. Graf, Phys. Rev. Lett. **98**, 036402 (2007); M. Nicklas, O. Stockert, Tuson Park, K. Habicht, K. Kiefer, L. D. Pham, J. D. Thompson, Z. Fisk, and F. Steglich, Phys. Rev. B **76**, 052401 (2007); A. Aperis, G. Varelogiannis, and P. B. Littlewood, Phys. Rev. Lett. **104**, 216403 (2010); for the spin-susceptibility behavior see, A. Aperis, G. Varelogiannis, P. B. Littlewood, and B. Simons, J. Supercond. Novel Magn. **22**, 115 (2009); for phenomenological discussion see, K. Miyake, J. Phys. Soc. Jpn. **77**, 123703 (2008); M. Mierzejewski, A. Ptok, and M. M. Maska, Phys. Rev. B **80**, 174525 (2009); Y. Yanase and M. Sigrist, J. Phys. Soc. Jpn. **78**, 114715 (2009).

[17] For didactical comparison of the two mechanisms see J. Spałek, Acta Phys. Pol. A **111**, 409 (2007).

[18] J. R. Schrieffer and P. A. Wolff, Phys. Rev. **149**, 491 (1966).

[19] I. T. Padilha and M. A. Continentino, Physica B **404**, 2920 (2009); F. D. Neto, M. A. Continentino, and C. Lacroix, J. Phys.: Condens. Matter **22**, 075701 (2010).

[20] O. Bodensiek, T. Pruschke, and R. Žitko, J. Phys.: Conf. Ser. **200**, 012162 (2010).

[21] H. Shimahara, Phys. Rev. B **50**, 12760 (1994); A. I. Buzdin and J. P. Brison, Europhys. Lett. **35**, 707 (1996).

[22] A. M. Clogston, Phys. Rev. Lett. **9**, 266 (1962); L. W. Gruenberg and L. Gunther, *ibid.* **16**, 996 (1966); K. Maki and T. Tsuneto, Prog. Theor. Phys. **31**, 945 (1964).

[23] T. Koponen, J. Kinnunen, J.-P. Martikainen, L. M. Jensen, and P. Törmä, New J. Phys. **8**, 179 (2006).

[24] J. Kaczmarczyk and J. Spałek, Phys. Rev. B **79**, 214519 (2009), and references therein.

[25] J. Kaczmarczyk and J. Spałek, arXiv:0907.3589, J. Phys.: Condens. Matter (to be published).

[26] Previous studies of 2D systems encompass the works: H. Burkhardt and D. Rainer, Ann. Phys. **506**, 181 (1994); K. Maki and H. Won, Czech. J. Phys. **46**, 1035 (1996); H. Shimahara, J. Phys. Soc. Jpn. **67**, 736 (1998); K. Yang and S. L. Sondhi, Phys. Rev. B **57**, 8566 (1998); A. B. Vorontsov, J. A. Sauls, and M. J. Graf, *ibid.* **72**, 184501 (2005). In all those papers the mass was spin independent. Also, in the spirit of BCS theory, the chemical potential was not readjusted in the superconducting states, an important factor in the case of very narrow-band correlated systems.

[27] H. Shimahara and S. Hata, Phys. Rev. B **62**, 14541 (2000).

[28] J. Jędrak and J. Spałek, Phys. Rev. B **81**, 073108 (2010).

[29] For recent review see, P. Monthoux, D. Pines, and G. G. Lonzarich, Nature (London) **450**, 1177 (2007), and references therein.